Canadian Journal of Pure and Applied Sciences
Vol. 15, No. 2, pp. 5253-5259, June 2021
Online ISSN: 1920-3853; Print ISSN: 1715-9997
Available online at www.cjpas.net

GRAVITY LEVELS COMPUTED FROM REFRACTIVE INDICES DISPLAYED BY POWDERED-ROCK FRAGMENTS

Stephen Arthur Langford
Langford Consulting, Danielson, Connecticut, USA

ABSTRACT

Refractive-index (RI) data are used to model gravity (*g*, gals) levels displayed by powdered-rock fragments. The base *g* level at each of two laboratories, were regressed with case (and other) weighting of 696 cases; representing all but two (2) of the 698, in which a total of 76,798 fragment RIs were compared to those of immersion liquids.

Keywords: Refractive index, refractivity, gravity, rock, powder, fragments, regression, modeling.

INTRODUCTION

The purpose here is to test the hypothesis that gravity might affect RIs. Then too, to test whether RIs displayed by rock-powder fragments can be used to model gravity levels related to sample fragments. To be clear: The *g* (gals) levels relate not to the gravities at data-collection laboratory sites; but first, in this experiment, to a base-level surface that has been averaged with case weighting, between the two laboratory-site *g* levels. Thereafter, however, the Predicted, Residuals, and Residuals-to-Residuals Models developed in this work pertain to the relative *g* levels created by how much of each kind of matter exists, at each location on the (RI,**λ**•nm) Emmons Surface.

The RI data were collected, between 23 October 1977 and 10 November 1993, while studying a powdered gabbro rock sampled from Ukumehame Valley, West Maui, Hawai'i. Because those labs were at significantly different elevations, the question as to whether gravity values (*g*, gals; m•s^2) might have affected RI-probability (%) results seemed to be worthy of investigation.

These three previous papers have presented:

1) the fundamental methodology employed for studying RIs displayed by mineral or rock powders, statistically significant results from study of fragments in whatever position they are first encountered; and, some calculations related to the mass (*m*), energy (E), and Weight (W) of an assumed vacuum structure at rest (Langford, 2021a).
2) Predicted and Residuals Models – based **only** upon the Quantum-Mechanical (QM) aspects and not involving any RI data – are presented; for rest mass (*m*), energy (*E*), and weight (*W*) (Langford, 2021b).
3) how RI probability levels correlate with prior works of Galileo, Newton, Einstein, Planck, and de Broglie; and how applications of Quantum Mechanical Theory mesh seamlessly with Real-World RI data (Langford, 2021c).

THE EXPERIMENT

Laboratory elevations in Honolulu, Hawai'i, and Oro Valley, Arizona, were significantly different. Rough estimations of gravity to be expected at each location were based upon the respective latitudes and elevations estimated with the aid of Google Earth Pro v.7.3.3.7786 (64-bit). They were calculated as *g* (gals•m•s^2) via https://www.sensorsone.com/local-gravity-calculator/.

The estimated values of *g* were then regressed against three degrees each of microscope-stage temperatures, estimated temperatures inside powder fragments, and the RI-probability statistic **(*L%+E%*)**, which was presented in (Langford, 2021a). Three weighting factors were included in the regression.

After RIs were found to be affected by gravity levels, it was possible to model gravity levels within the powder fragments. For the data at each lab, correction factors were developed and applied to the original *g* estimates. Predicted, Residuals, and Residuals of Residuals Models were then created and are presented below.

RESULTS

Initial gravity (*g*) estimations

The Honolulu, Hawai'i, lab latitude was estimated to be 21.298547N; its elevation was estimated to be about 25 meters. The Oro Valley, Arizona, lab latitude was

Corresponding author e-mail: gambist@gmail.com

estimated to be 32.372913N; its elevation was estimated to be about 796 meters. Those values resulted in 0.978707 gal and 0.979269 gal calculations of *g*, respectively.

Gravity estimates regressed against 12 independent variables

In the **Appendix**, Figure 1 shows the most-germane regression results reported by SAS JMP Pro v.15.2.1.

Gravity correction factors, Honolulu and Oro Valley

The mean residual *g* value for the first 116 of the 696 total cases, derived from work in Hawai'i, is 4.5100910164062 $\times 10^{-5}$ gal; that for the rest of those cases, from work in Arizona, is 9.0870721451592 $\times 10^{-6}$. Those levels of precision derive from the fact that liquid RI estimations were rounded to the sixth decimal place as well as the fact that many more cases were created in Arizona than in Hawai'i. Those mean residual *g* values were applied as correction factors to the initial *g* estimates, for which the regression report comprises Figure 1.

Creation of Predicted, Residuals, and Residuals-of-Residuals *g* Models

In the **Appendix**, Figure 2 shows the perspective and plan views for each of the Predicted, Residuals, and Residuals-of-Residuals *g* Models.

A 243,137 KB version of Figure 2 is available at https://tinyurl.com/fhvffwuc. A 2,373 KB file showing the inset at lower right of Figure 2 is available at https://tinyurl.com/aul4am8p. The spike at RI 1.68608 has been seen in many previous models and will be discussed below.

DISCUSSION

My dear wife, Joann Kiomi Nakagawa, contended that for any statistical significance the elevations initially used in the regression reported in Figure 1 should have been from at least eight (8) different locations. Though the author honors the maxim that for statistical significance one needs at least eight (8) samples, the author also contends that this is a pioneering, reconnaissance study; that others interested in the approach can gather data from as many geographical locations as they like; and that – given the 696 cases created while classifying 76,798 fragments in the study – the so-called whitewash effect (the author can't recall where the author first read that term) of statistics more than compensates (for present purposes) for the statistical weakness to which she points.

Results continue to demonstrate what might be called the fractal nature of the data. It might well be that a fractal approach to the data would more swiftly result in better and faster analytical comprehension. But – given the Gaussian approach to so many different minerals, mineraloids, glasses, and opaques (which might at times become transparent due to strong overtone and undertone resonances) – the routine modeling of gravity residual data at ever-finer orders of magnitude (even unto the milligals or microgal level) would be quite a reasonable approach for any others who might want to apply such statistical approaches to emulate, as provided by such tools as GLM …before going on to discover what other approaches might improve statistical results.

The spike at about 589.3 nm and RI 1.68608 (Inset, Fig. 2) might be important, but pinning down what mineral is involved has not yet been possible. The 2.42_{Na} RI listed (Larsen and Berman, 1934) for Magnetite is far from that peak RI of 1.68608, and no other Spinel listed in their Table 20 comes closer than the RI 1.718 that they list for pure Spinel. On the other hand, overtones and undertones may be so strong that one of the Spinels resonates in RI at 1.68608; and that most probably would be from Magnetite. Because Magnetite is thought to be the predominant ore mineral in subject gabbro Sample FUD27, and because this writer has thought that magnetic particles might form coherent threads through a cooling magma, maybe forming a 3D network that is both electrically and thermally conductive; and because such conductivity might well transfer energy in either direction – whether from a cooling magma chamber or a lightning strike; the roles that Magnetite plays in magmas and rocks seems to merit further consideration. What roles might it play in outer space?

Total-*g* Model = Predicted + Residuals + Residuals-of-Residuals Models

The three Models shown in Figure 2 were summed to create the Total-*g* Model shown in Figure 3 in the **Appendix**. Initially, the Total-*g* Model was disappointing, because it so closely resembles the Predicted Model of Figure 2. However, when it was "flown" in the 3D mode of Surfer®20, striking details never before available became apparent, as shown in Figure 4 in the **Appendix**.

CONCLUSION

Gravity levels, at locations where RI data are collected, **do** appreciably affect displayed RI values. And RI data can be used to model gravity levels among rock-powder fragments. The base level for modeled *g* (gals) levels is set by case-weighted averaging of *g* levels estimated at each of the two laboratories used during data collection. But the Predicted, Residuals, and Residuals-to-Residuals Models developed in this work pertain to the relative *g* levels created by how much of each kind of matter exists in the sampled powder, at each location on the (RI,**λ**•nm) Emmons Surface.

No direct correlation seems to exist between this approach to gravity and that of free-air and Bouguer-anomaly analyses, because the background surface against which *g* values are measured is arbitrary, has nothing really much to do with where the laboratories were actually located, and has no relation at all to local variabilities due to such factors as nearby mountains, trenches, or terrains with varying specific gravities among surrounding rocks. Freed from such considerations, the approach makes for an eminently good way to map gravity effects among all the constituents in a powdered gabbro sample; it could also be used for other rock and mineral samples.

The question as to how best to estimate volume – so that density (grams per cc) estimates could be made – is tantalizing; because it would be fun to be able to calculate the so-called "specific refractive energy" (which seems not to be directly related to the E of $E = mc^2$), as defined by the Law of Gladstone and Dale (Gladstone and Dale, 1863; Larsen and Berman, 1934, p. 30, ff.); wherein (noting that n = RI, K is specific refractive energy, and d is density [g/cc]): $K = (n - 1)/d$; (where n is RI assumed to be at 25°C for $\lambda = 589.3$ nm, unless otherwise stated).

WORK LOGS

Work logs related to the development of this paper are posted at https://tinyurl.com/4d8nthst.

ACKNOWLEDGEMENT

The author thanks Pedro Leo E. Contreras for contributing several important suggestions for improvement to early drafts of this paper. Other, comprehensive acknowledgments are provided at https://tinyurl.com/qt20n48o.

REFERENCES

Gladstone, JH. and Dale, TP. 1863. Researches on the refraction, dispersion, and sensitiveness of liquids. Philosophical Transactions of the Royal Society of London. 153:337-343. https://www.jstor.org/stable/108799, https://www.jstor.org/stable/pdf/108799.pdf?refreqid=excelsior%3Aaa7f88f10e968298dd1441797b77aea3

Langford, SA. 2021[a]. Refractive index, a key to better petrography and to fundamental laws of Nature; *m*, *E*, and *W* Vacuum-Structure rest-mass calculations. Canadian Journal of Pure and Applied Sciences. 15(1):5133-5140.

Langford, SA. 2021[b]. A portion of Vacuum-Structure mass, energy, and weight. Canadian Journal of Pure and Applied Sciences. 15(1):5169-5178.

Langford, SA. 2021[c]. Weight, mass, energy, temperatures, permittivity, permeability, and chemistry determine refractive indices. Canadian Journal of Pure and Applied Sciences. 15(2):In Press.

Larsen, ES. and Berman, H. 1934. The Microscopic Determination of the Nonopaque Minerals. 2nd edition. Eds. Larsen, ES. and Berman, H. USGS Bulletin 848, Government Printing Office, Washington D.C., USA. pp. 266. https://pubs.usgs.gov/bul/0848/report.pdf

Received: Feb 9, 2021; Accepted: April 12, 2021

Appendix 1. Figures 1, 2, 3, and 4 mentioned in the context above.

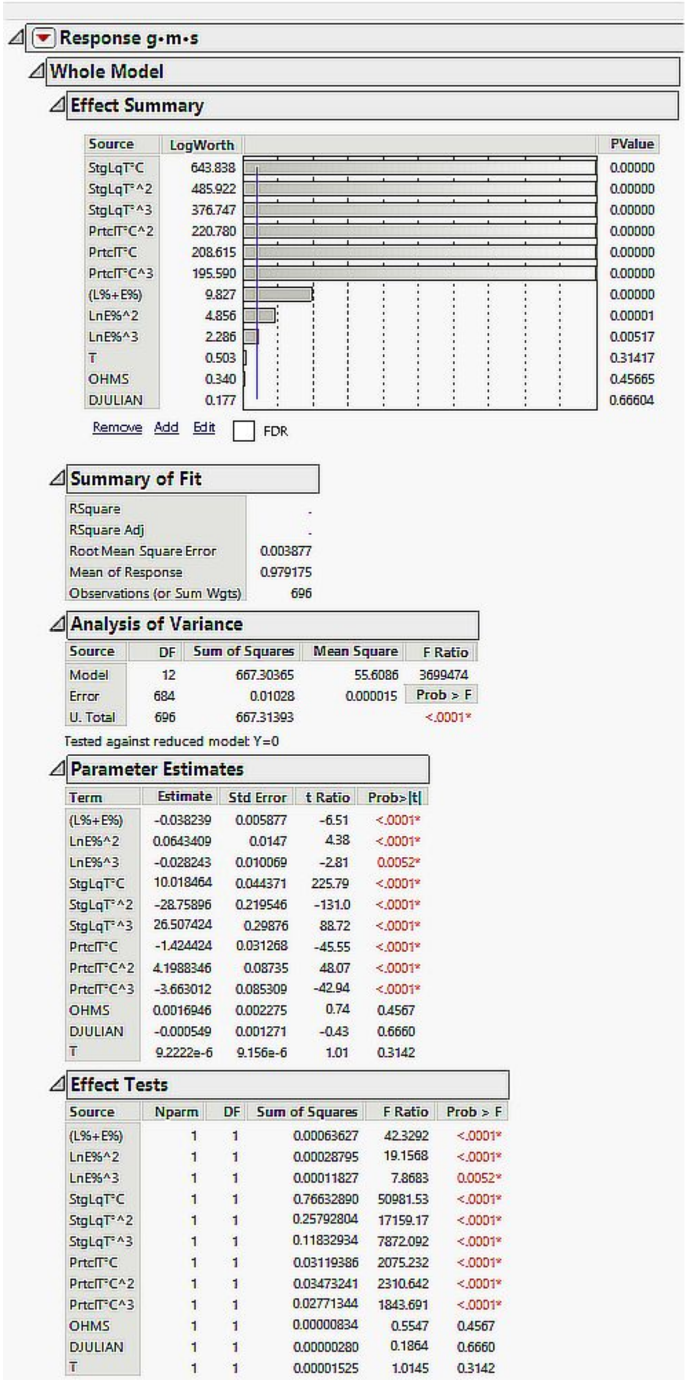

Response g•m•s

Whole Model

Effect Summary

Source	LogWorth	PValue
StgLqT°C	643.838	0.00000
StgLqT°^2	485.922	0.00000
StgLqT°^3	376.747	0.00000
PrtclT°C^2	220.780	0.00000
PrtclT°C	208.615	0.00000
PrtclT°C^3	195.590	0.00000
(L%+E%)	9.827	0.00000
LnE%^2	4.856	0.00001
LnE%^3	2.286	0.00517
T	0.503	0.31417
OHMS	0.340	0.45665
DJULIAN	0.177	0.66604

Remove Add Edit FDR

Summary of Fit

RSquare	.
RSquare Adj	.
Root Mean Square Error	0.003877
Mean of Response	0.979175
Observations (or Sum Wgts)	696

Analysis of Variance

Source	DF	Sum of Squares	Mean Square	F Ratio
Model	12	667.30365	55.6086	3699474
Error	684	0.01028	0.000015	Prob > F
U. Total	696	667.31393		<.0001*

Tested against reduced model: Y=0

Parameter Estimates

Term	Estimate	Std Error	t Ratio	Prob>|t|
(L%+E%)	-0.038239	0.005877	-6.51	<.0001*
LnE%^2	0.0643409	0.0147	4.38	<.0001*
LnE%^3	-0.028243	0.010069	-2.81	0.0052*
StgLqT°C	10.018464	0.044371	225.79	<.0001*
StgLqT°^2	-28.75896	0.219546	-131.0	<.0001*
StgLqT°^3	26.507424	0.29876	88.72	<.0001*
PrtclT°C	-1.424424	0.031268	-45.55	<.0001*
PrtclT°C^2	4.1988346	0.08735	48.07	<.0001*
PrtclT°C^3	-3.663012	0.085309	-42.94	<.0001*
OHMS	0.0016946	0.002275	0.74	0.4567
DJULIAN	-0.000549	0.001271	-0.43	0.6660
T	9.2222e-6	9.156e-6	1.01	0.3142

Effect Tests

Source	Nparm	DF	Sum of Squares	F Ratio	Prob > F
(L%+E%)	1	1	0.00063627	42.3292	<.0001*
LnE%^2	1	1	0.00028795	19.1568	<.0001*
LnE%^3	1	1	0.00011827	7.8683	0.0052*
StgLqT°C	1	1	0.76632890	50981.53	<.0001*
StgLqT°^2	1	1	0.25792804	17159.17	<.0001*
StgLqT°^3	1	1	0.11832934	7872.092	<.0001*
PrtclT°C	1	1	0.03119386	2075.232	<.0001*
PrtclT°C^2	1	1	0.03473241	2310.642	<.0001*
PrtclT°C^3	1	1	0.02771344	1843.691	<.0001*
OHMS	1	1	0.00000834	0.5547	0.4567
DJULIAN	1	1	0.00000280	0.1864	0.6660
T	1	1	0.00001525	1.0145	0.3142

Fig. 1. The independent variable **g•m•s** (standing for *g* and later renamed to **g•m•s^2**) was regressed in a mode simulating GLM (General Linear Modeling). Variable ***(L%+E%)*** tracks RI probability levels; **StgLqT°C** tracks temperatures set for the microscope stage and assumed to be immersion-liquid temperatures; **PrtclT°C** tracks temperatures estimated to be interior to fragments; 2^{nd}-degree and 3^{rd}-degree variables for each of those were included as independent variables. Weighting variables **OHMS**, **DJULIAN**, and **T**, respectively compensate for catastrophic system changes, drift (gradual system changes through time), and case weighting; although their necessary effects do not seem to be fully appreciated by the report; taken altogether, they probably merit a red-colored Prob > *F*.

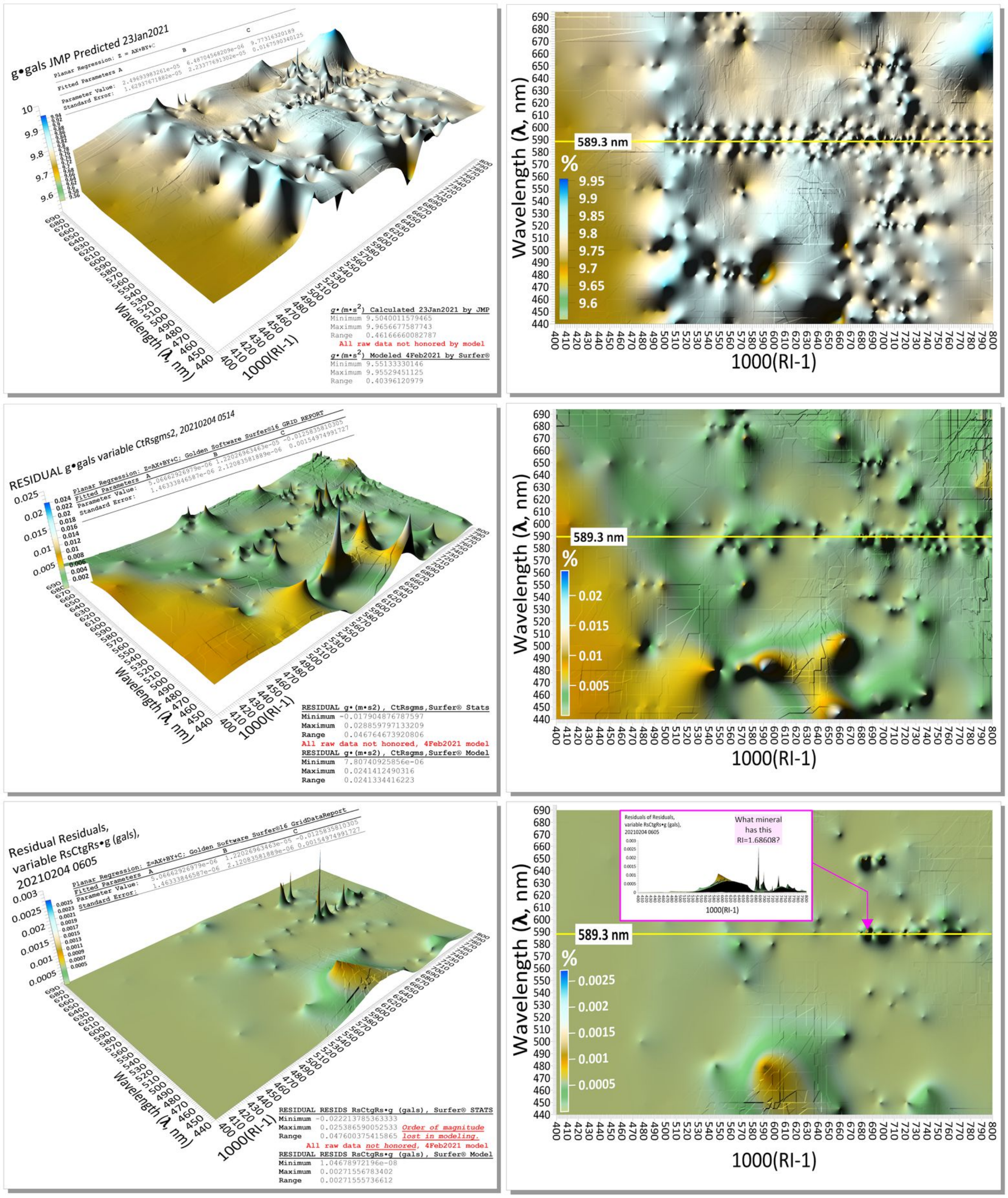

Microscopical Free-Air & Bouguer Anomalies, or what?

Fig. 2. The perspective and plan views for each of the Predicted, Residuals, and Residuals-of-Residuals *g* Models.

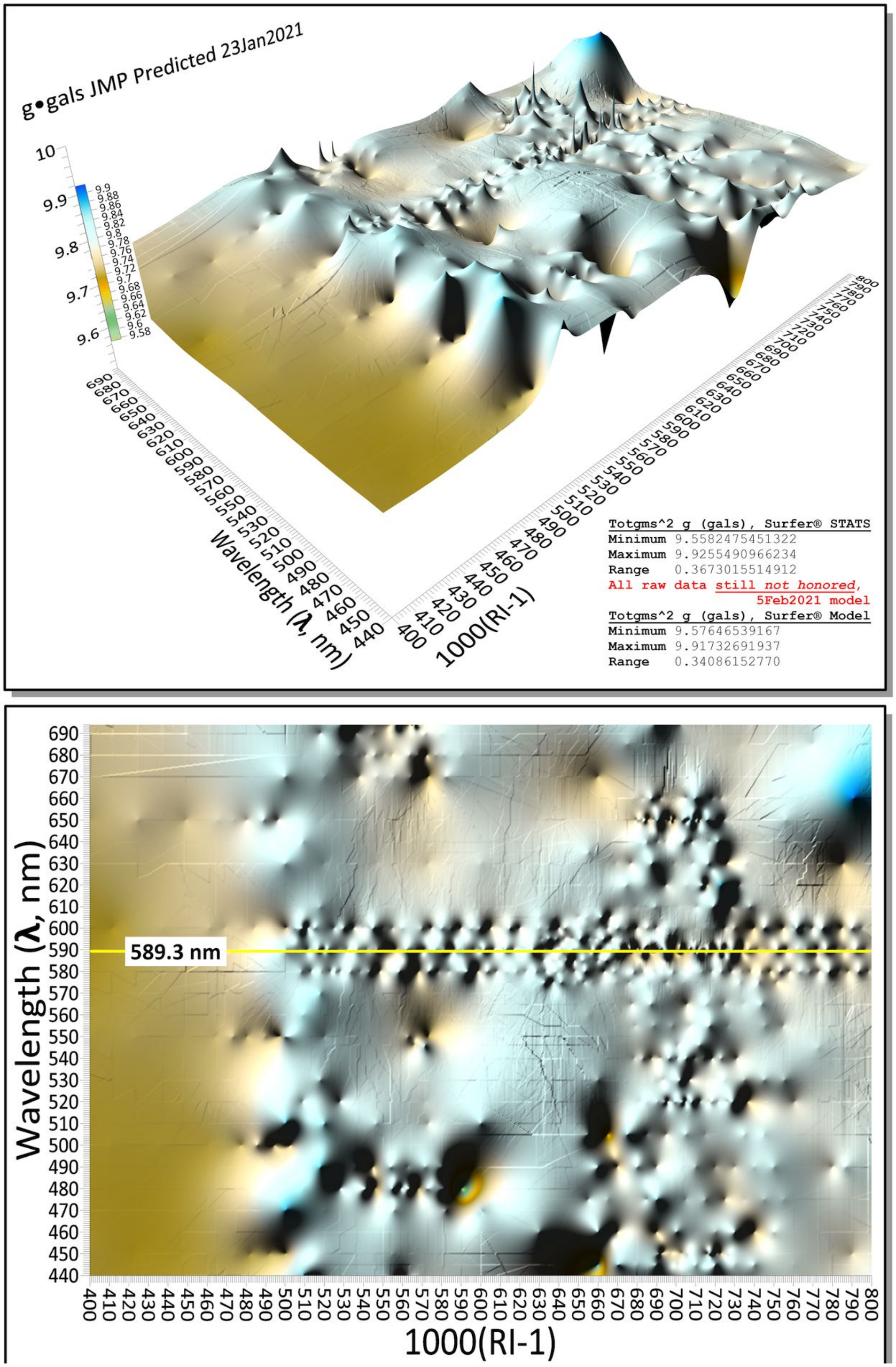

Fig. 3. The plan view of Total-*g* Model. A very-high-resolution version of this figure is available at https://tinyurl.com/efhyb886.

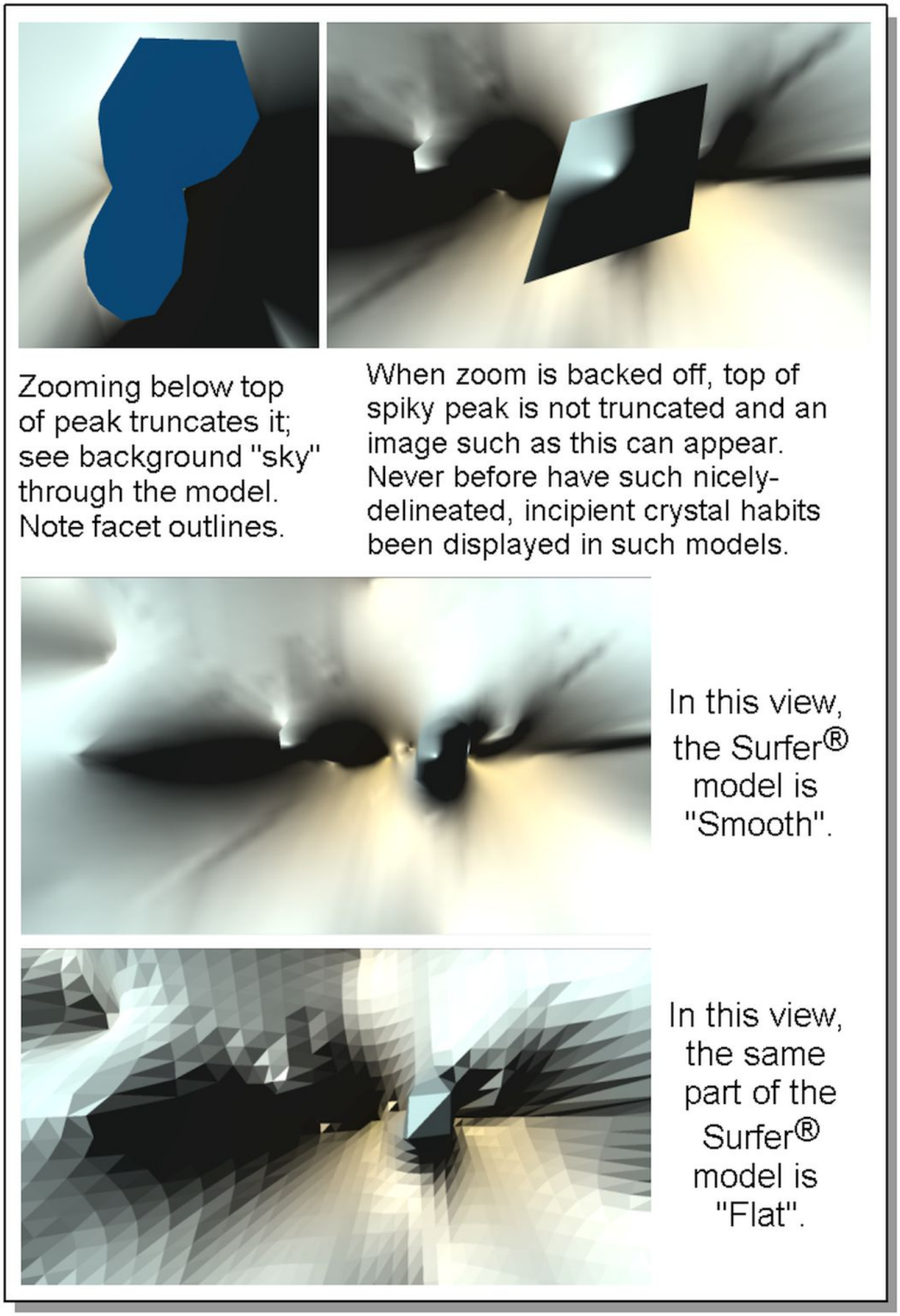

Fig. 4. The best model resolutions to date. Readers new to this work must be reminded that these are not photographs of real things. They are screen shots of modeled data.